land

MDPI

Article

Spatio-Temporal Variation and Drivers of Land-Use Net Carbon Emissions in Chengyu Urban Agglomeration, China

Wen Wang [1], Xin Wang [1,2,3,*], Li Wang [4], Zhihua Zhang [1] and Daren Lyu [1,2,3]

[1] Key Laboratory of Middle Atmospheric and Global Environment Observation, Institute of Atmospheric Physics, Chinese Academy of Sciences, Beijing 100029, China; wangwen@mail.iap.ac.cn (W.W.); zhangzhihua@mail.iap.ac.cn (Z.Z.); ludr@mail.iap.ac.cn (D.L.)
[2] Key Laboratory of Atmospheric Environment and Extreme Meteorology, Chinese Academy of Sciences, Beijing 100029, China
[3] China College of Earth and Planetary Sciences, University of Chinese Academy of Sciences, Beijing 100049, China
[4] Key Laboratory of Remote Sensing and Digital Earth, Aerospace Information Research Institute, Chinese Academy of Sciences, Beijing 100101, China; wangli@aircas.ac.cn
* Correspondence: wangx2003@mail.iap.ac.cn

Abstract: Land-use change is an important cause of carbon emissions (CEs). In the context of achieving carbon peaking and carbon neutrality goals, understanding the coupling mechanisms between land-use change and CEs is of great significance for fostering regional low-carbon sustainable development. In this study, the land-use net carbon emissions (LCN) calculation and evaluation model was built based on the perspective of land-use change. The land-use variation matrix, standard deviation ellipse, and spatial autocorrelation analysis were used to analyze the spatio-temporal evolution of land-use and the LCN in the Chengyu urban agglomeration (CUA) from 2000 to 2020. Meanwhile, the economic contribution coefficient and ecological support coefficient were applied to evaluate the alignment among the CEs, socio-economic development, and the ecological environment. In addition, the modified Kaya and Logarithmic Mean Divisia Index (LMDI) models were used to quantitatively analyze the drivers and underlying influence mechanisms of the LCN. The results showed the following: (1) The area of built-up land and forest land expanded rapidly, mainly transforming grassland and farmland to built-up land and forest land in the CUA during the study period. The built-up land was the main source of the regional CEs. The land-use changes led to the migration of the LCN center and the variations in spatial clustering. (2) The growth rate of the LCN decreased after 2010, and the disparities in carbon productivity and the carbon compensation rate among the cities gradually narrowed from 2000 to 2020. The alignment among the regional CEs, socio-economic development, and ecological environmental governance was effectively improved. (3) The economic development level and energy consumption intensity were the primary facilitator and inhibitor of the LCN, respectively. The results could offer valuable references and insights for formulating regional carbon reduction strategies and policies.

Keywords: city agglomeration; land-use; carbon emissions; spatio-temporal pattern; LMDI

check for updates

Citation: Wang, W.; Wang, X.; Wang, L.; Zhang, Z.; Lyu, D. Spatio-Temporal Variation and Drivers of Land-Use Net Carbon Emissions in Chengyu Urban Agglomeration, China. *Land* **2024**, *13*, 2160. https://doi.org/10.3390/land13122160

Academic Editor: Marko Scholze

Received: 6 November 2024
Revised: 3 December 2024
Accepted: 10 December 2024
Published: 11 December 2024

Copyright: © 2024 by the authors. Licensee MDPI, Basel, Switzerland. This article is an open access article distributed under the terms and conditions of the Creative Commons Attribution (CC BY) license (https://creativecommons.org/licenses/by/4.0/).

1. Introduction

Land-use and land-cover change significantly impacts climate change and the carbon cycle of terrestrial ecosystems. It is the second largest contributor to carbon emissions after energy consumption, as it is responsible for one-third of human-induced carbon emissions [1,2]. In 2019, the Intergovernmental Panel on Climate Change (IPCC) highlighted the correlation between land-use and carbon emissions in the special report on Climate Change and Lands [3]. When compared to the Fifth Assessment Report of the IPCC [4], the Sixth Assessment Report placed greater emphasis on land-use change and carbon emissions [5]. Research on carbon emissions from a land-use perspective has emerged as a

contemporary research hotspot [6–10]. The related research primarily focuses on the carbon emissions calculation, the characteristics of spatial patterns, the influencing factors, and the future carbon emissions projections. The quantitative calculation of carbon emissions is the basis of low-carbon policy research, encompassing land-use carbon sinks (CSs) and carbon emissions (CEs). Built-up land is the most significant CE land-use type. Research emphasis lies in indirectly calculating built-up land's CEs through the establishment of an energy consumption-based CEs model [11–13]. The land-use types primarily serving as CSs include forest land, grassland, water area, and unused land. The CS potential of these areas is often calculated using the carbon sequestration coefficient method [14–16]. There is still controversy about whether farmland should be classified as a CS or CE land-use type. Some scholars argued that farmland acts as a source of emissions, as it could generate CEs during crop cultivation activities. Consequently, farmland should be excluded from CS calculations [12,14]. However, it has been pointed out that farmland has important CS potential, as indicated in the IPCC report [17]. The Gini coefficient, spatial autocorrelation, the coefficient of variation, and the standard deviation ellipse are often employed in spatial pattern studies to assess spatial correlation and the heterogeneity of CEs [15,18–20]. Regarding the studies on the drivers of land-use CEs, economic development levels, population scale, industrial structures, energy intensity, technology levels, etc., are the commonly considered ones, and the widely used methods include an input–output analysis, and the Logarithmic Mean Divisia Index (LMDI) model [21–25]. In prediction studies, a neural network analysis, the LEAP model, and the STIRPAT model are frequently utilized to determine the feasibility of low-carbon development and meet energy conservation and emission reduction targets on schedule [26–29].

Generally, scholars have achieved notable strides in the field of land-use CEs research, adopting a growing array of methodologies and yielding a plethora of insightful findings. However, there are still certain limitations that remain unaddressed. First, previous research has primarily concentrated on macro scales or independent administrative entities, such as national and provincial regions, and the majority of studies have focused on short-term CEs, with limited research dedicated to the long-term dynamics of CEs in cities and urban agglomerations with cross-administrative boundaries. Second, in the process of CEs calculations, farmland has been predominantly perceived solely as a CE or CS land-use type, without considering its dual functional attributes, which may result in inaccuracies within the studies. Furthermore, the economically advanced eastern provinces of China have been widely focused on and studied, while the western regions, emerging as a new growth pole for China's economy, have garnered comparatively less research attention. Moreover, there is a significant dearth of thorough and systematic inquiries into the non-equilibrium of the spatio-temporal characteristics, the heterogeneity of drivers, and the underlying influence mechanisms of regional CEs.

Therefore, the research object of this study was the Chengyu urban agglomeration (CUA), which contains 22 prefecture-level cities and is known as the core engine of economic development in southwest China. The land-use data, carbon emission database (ODIAC), agricultural production data, as well as socio-economic data were applied to build the land-use net carbon emissions (LCN) calculation and evaluation model from the perspective of land-use change. The main objectives are as follows: (1) To study the spatio-temporal evolution characteristics of land-use change and the LCN in the CUA from 2000 to 2020. (2) To assess the alignment among the CEs, socio-economic development, and the ecological environment. (3) To conduct a quantitative analysis of the drivers of the LCN and the underlying influence mechanisms, to offer scientific insights for developing CEs reduction strategies customized to local contexts and the sustainable development of the CUA (Figure 1).

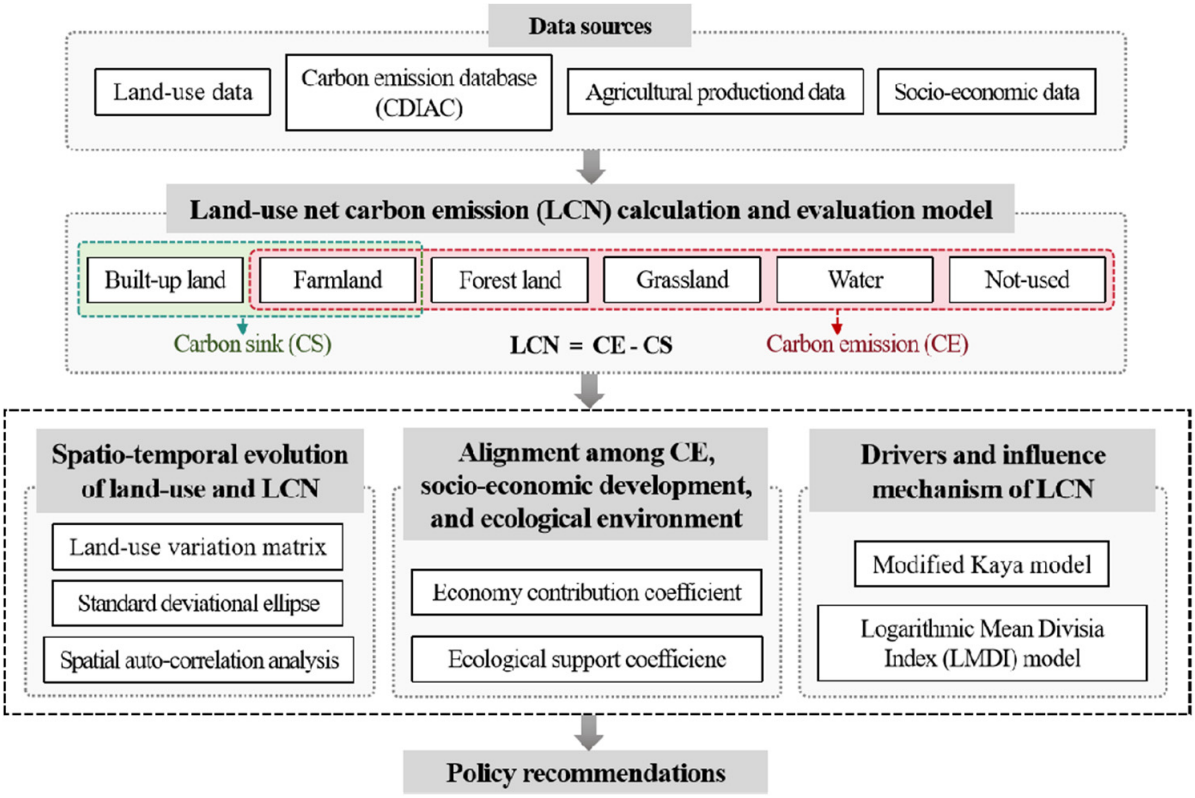

Figure 1. Research framework.

2. Materials and Methods

2.1. Study Area

The CUA is located in the upper Yangtze River (27°39′–33°03′ N, 101°56′–110°11′ E, Figure 2). It stands as the most economically developed urbanized region in western China. By 2022, the permanent resident population of the CUA accounted for 8.21% of China's total population, and its regional gross domestic product (GDP) contributed 7.17% to the national GDP. As a densely populated and rapidly developing inland region in China, the CUA has undergone significant land-use transformations in recent decades, which were accompanied by rising energy consumption levels and mounting environmental pressures. Consequently, the LCN driven by land-use changes across 22 prefecture-level cities within the CUA were studied. To better capture the heterogeneity among various agglomeration areas, the CUA was subdivided into six regions, categorized by their development levels and industrial profiles. The six regions were: (1) Chongqing; (2) the Chengdu Plain Economic Zone (CDP-EZ), including Chengdu, Deyang, Mianyang, Suining, Ziyang, Meishan, Leshan, and Ya'an; (3) the Northeast Sichuan Economic Zone (NES-EZ), including Guangyuan, Nanchong, Guang'an, Dazhou, and Bazhong; (4) the Southern Sichuan Economic Zone (SS-EZ), including Neijiang, Zigong, Yibin, and Luzhou; (5) the Southwest Sichuan Economic Zone (SWS-EZ), including Panzhihua and the Liangshan Yi Autonomous Prefecture (Liangshan); (6) the Northwest Sichuan Ecological Demonstration Zone (NWS-EDZ), including the Ngawa Tibetan and Qiang Autonomous Prefecture (Ngawa) and the Garze Tibetan Autonomous Prefecture (Garze).

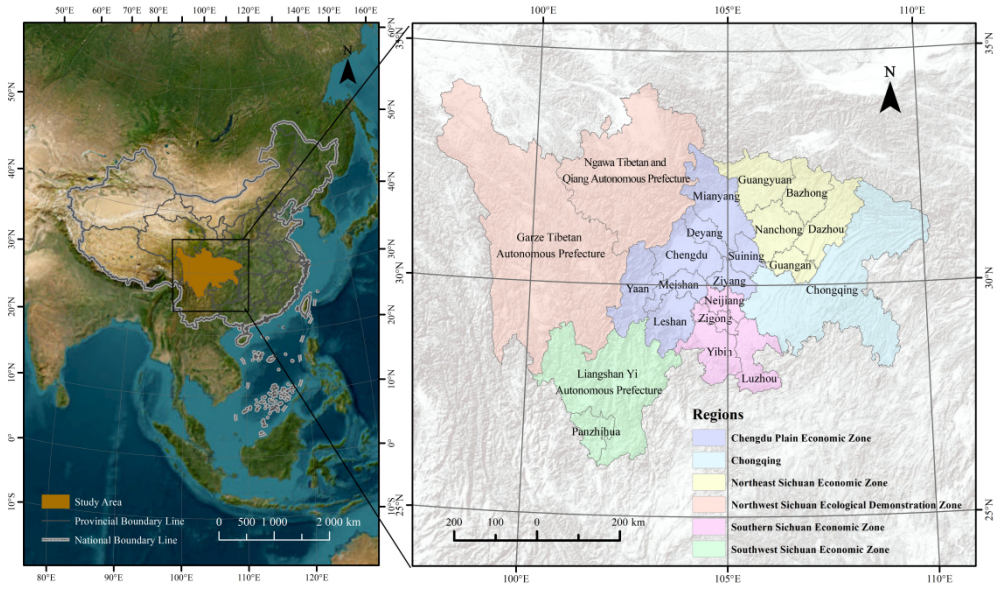

Figure 2. Geographical location and administrative division of the study area.

2.2. Data Source and Processing

The land-use remote sensing monitoring dataset (CNLUCC), encompassing the years 2000, 2005, 2010, 2015, and 2020, was provided by the Data Center for Resources and Environmental Sciences (http://www.resdc.cn/, accessed on 25 April 2024). The land-use data were resolved at a 1 km × 1 km grid scale. According to the secondary classification system in the CNLUCC, the data were classified into six primary categories and 25 subcategories. The six primary categories are farmland, forest land, grassland, water, built-up land, and unused land. The data on the GDP, population, energy consumption, and agricultural production activities for the specific years (2000, 2005, 2010, 2015, and 2020) were sourced from the respective statistical yearbooks of the Sichuan Province, Chongqing, and the cities within the CUA. The Open-source Data Inventory for Anthropogenic Carbon Dioxide (ODIAC) serves as a high-spatial resolution dataset detailing the global carbon dioxide emissions from fossil fuel combustion, cement production, and gas flaring. The latest version (ODIAC2020B) with a spatial resolution of 1 km × 1 km was applied in this study (https://db.cger.nies.go.jp/, accessed on 28 May 2024).

2.3. Methodology

2.3.1. LCN Calculation

- CEs from built-up land

Built-up land serves as the primary platform for human activities. Drawing from the 2006 IPCC Guidelines for National Greenhouse Gas Inventories and the relevant literature [12,30,31], the primary sources of CEs from built-up land are energy consumption, industrial processes, and respiration by humans and livestock. The calculation formula is presented below:

$$CE_{bul} = CE_{fue} + CE_{ind} + CE_{peo/ani} \quad (1)$$

where CE_{bul}, CE_{fue}, CE_{ind}, and $CE_{peo/ani}$ refer to the CEs from built-up land, energy consumption, industrial processes, and respiration by humans and livestock, respectively.

Data on the energy consumption and industrial processes of several cities in the CUA were unavailable. Consequently, the ODIAC emissions data were utilized to represent the CE_{fue} + CE_{ind}. Regarding the $CE_{peo/ani}$, the focus was primarily on humans and large livestock, such as pigs, cattle, and sheep. The calculation formula is as follows:

$$CE_{peo/ani} = \sum_{i=1}^{4} P_i \times a_i \quad (2)$$

where P_i represents the permanent population of each city or the quantity of livestock at a year's end, and a_i represents the corresponding coefficient (Table 1).

Table 1. Carbon emission coefficients.

Land-Use Type	Carbon Emission Component	Note	Coefficient	Unit	Reference
Built-up land	Respiration of humans	α_1	0.079	t C/(yr·person)	[12,30]
	Respiration of pigs	α_2	0.082	t C/(yr·head)	
	Respiration of cattle	α_3	0.077	t C/(yr·head)	
	Respiration of sheep	α_4	0.041	t C/(yr·head)	
Farmland	Fertilizers	b_1	0.858	kg C/kg	[12]
	Crop cultivation	b_2	16.47	kg C/hm2	[12,31]
	Farming machinery	b_3	0.18	kg C/kW	
	Irrigation	b_4	266.48	kg C/hm2	

- CEs from farmland

Farmland primarily acts as an emission source due to crop cultivation activities [32]. The CEs from fertilizers, crop cultivation, farming machinery, and irrigation should be taken into account. The calculation formula is as follows:

$$CE_{cul} = \sum_{i=1}^{4} K_i \times b_i \quad (3)$$

where K_i represents the amount of fertilizer applied, the crop cultivation area, the electricity consumption of farming machinery, or the irrigation area for each city. b_i represents the corresponding coefficient (Table 1).

- CSs from farmland, forest land, grassland, water area, and unused land

The land-use types that function in CSs include forest land, grassland, water areas, and unused land. In addition, farmland also has the capacity of CS, which is reflected in both crops and soils. The effect of crop CSs was often overlooked in previous studies due to the short harvest period [15,33]. Consequently, this study focused solely on the CSs of farmland soils. The CSs from various land-use types were determined using a coefficient method, as referenced in the related literature [14–16,34–36]. The formula is as follows:

$$CS = \sum_{i=1}^{13} A_i \times \beta_i \quad (4)$$

where CS refers to the carbon sinks of all the land-use types. A_i represents the area of various land-use types, and β_i represents the corresponding coefficient (Table 2).

Table 2. Carbon sequestration coefficients.

Land-Use Type		Note	Coefficient /t C·(hm^2·yr)	Reference
Category	Sub-Category			
Farmland	/	β_1	0.553	[15]
Forest land	Forest	β_2	0.87	[14,15,34]
	Shrub land	β_3	0.23	
	Open woodland	β_4	0.58	[14,15]
	Other woodland	β_5	0.233	
Grassland	High coverage grassland	β_6	0.138	[14,15]
	Medium coverage grassland	β_7	0.046	
	Low coverage grassland	β_8	0.021	
Water	River and canals	β_9	0.671	[14,35]
	Lakes	β_{10}	0.303	
	Reservoirs and ponds	β_{11}	0.303	
	Shoals	β_{12}	0.567	[14]
Unused	/	β_{13}	0.005	[16,36]

- LCN

The total quantity of CEs surpassed that of CSs within the CUA. The regional carbon balance, denoted as LCN, is calculated as follows:

$$LCN = CE_{bul} + CE_{cul} - \sum CS \tag{5}$$

2.3.2. Construction of Land-Use Variation Matrix

A two-dimensional land-use variation matrix was created to illustrate the transformation of land-use types from the start to the end of the study period. The matrix quantified the changes through a superimposition across various time points, as detailed below:

$$B_{ij} = \begin{bmatrix} B_{11} & B_{11} & \dots & B_{1n} \\ B_{21} & B_{21} & \dots & B_{2n} \\ \vdots & \vdots & \ddots & \vdots \\ B_{n1} & B_{n2} & \dots & B_{nn} \end{bmatrix} \tag{6}$$

where B_{ij} denotes the area transformed from land-use type i to type j, and n signifies the total number of land-use types under consideration.

2.3.3. Analysis of the Spatial Pattern Changes

Leveraging the spatial analysis capabilities of ArcGIS 10.8, the spatial distribution of the LCN was analyzed using the standard deviation ellipse (SDE). The long-half axis and area of the ellipse represent the primary direction and the degree of agglomeration (dispersion) for the dataset distribution, respectively.

Based on the local spatial autocorrelation analysis function of ArcGIS 10.8, the spatial clustering characteristics of the LCN within the study area were quantified using the Moran's I Index. A positive Moran's I Index signifies that the regional LCN exhibits spatial clustering, whereas a negative Moran's I Index indicates that the LCN is significantly different from its surroundings. An index value of 0 suggests that the LCN is randomly distributed across the area.

2.3.4. Carbon Balance Analysis

A carbon balance analysis of the two aspects, namely the economic contribution coefficient (ECC) and the ecological support coefficient (ESC), provides an effective assessment of the alignment among the regional CEs, socio-economic development, and the ecological environment [25].

The ECC serves as a metric to evaluate the variance in regional CEs from the perspective of economic benefits, capturing the extent of regional CEs production. The definition formula is as follows:

$$ECC_i = \frac{GDP_i}{\sum GDP} / \frac{CE_i}{\sum CE} \tag{7}$$

where GDP_i and $\sum GDP$ represent the GDP of city i and the entire study region, respectively, CE_i and $\sum CE$ represent the CEs of city i and the study region, respectively. If the ECC is greater than 1, the economic contribution rate of city i to the study region exceeds its CEs contribution rate, indicating a higher CEs economic benefit. If the ECC is less than 1, it signifies a lower CEs economic benefit.

The ESC serves as an indicator of the carbon compensation rate, reflecting the fairness of a potential regional carbon ecological contribution. The definition formula is as follows:

$$ESC_i = \frac{CS_i}{\sum CS} / \frac{CE_i}{\sum CE} \tag{8}$$

where CS_i and $\sum CE$ represent the CSs of city i and the entire study region, respectively. If the ESC exceeds 1, the carbon compensation rate is high, otherwise it is low.

2.3.5. Driver Decomposition Method

The LMDI decomposition method was initially proposed by Ang [37], and has the advantages of straightforward operation, robust adaptability, and ensuring no residual decomposition [38]. Based on the extended Kaya model and the LMDI decomposition method, five factors were identified and decomposed: the energy utilization structure, the energy consumption intensity, the economic development level, the population density, and the built-up land scale [39–41]. The contributions of each driver for the LCN within the CUA were quantitatively analyzed.

The extended Kaya model is as follows:

$$CN = \frac{CN}{E} \times \frac{E}{GDP} \times \frac{GDP}{P} \times \frac{P}{A} \times A = u \times c \times e \times p \times a \quad (9)$$

where, $u = CN/E$ is the carbon emission per unit of energy consumption, representing the energy utilization structure. $c = E/GDP$ is the energy consumption per unit of the regional GDP, representing the energy consumption intensity. $e = GDP/P$ is the regional per capita GDP, representing the economic development level. $p = P/A$ is the population per unit area of built-up land, representing the population density. $a = A$ is the area of built-up land, representing the built-up land scale.

The additive decomposition method is used to decompose the five drivers. The process is as follows:

$$\Delta CN = CN^T - CN^0 = \Delta u + \Delta c + \Delta e + \Delta p + \Delta a \quad (10)$$

$$\Delta u = \sum_i \frac{CN_i^T - CN_i^0}{lnCN_i^T - lnCN_i^0} \times ln\frac{u^T}{u^0} \quad (11)$$

$$\Delta c = \sum_i \frac{CN_i^T - CN_i^0}{lnCN_i^T - lnCN_i^0} \times ln\frac{c^T}{c^0} \quad (12)$$

$$\Delta e = \sum_i \frac{CN_i^T - CN_i^0}{lnCN_i^T - lnCN_i^0} \times ln\frac{e^T}{e^0} \quad (13)$$

$$\Delta \mathrm{p} = \sum_{\mathrm{i}} \frac{\mathrm{CN_i^T} - \mathrm{CN_i^0}}{\mathrm{lnCN_i^T} - \mathrm{lnCN_i^0}} \times \mathrm{ln}\frac{\mathrm{p^T}}{\mathrm{p^0}} \quad (14)$$

$$\Delta \mathrm{a} = \sum_{\mathrm{i}} \frac{\mathrm{CN_i^T} - \mathrm{CN_i^0}}{\mathrm{lnCN_i^T} - \mathrm{lnCN_i^0}} \times \mathrm{ln}\frac{\mathrm{a^T}}{\mathrm{a^0}} \quad (15)$$

$$K_{u/c/e/p/a} = (\Delta u/c/e/p/a \div \Delta CN) \times 100\% \quad (16)$$

where Δu, Δc, Δe, Δp, and Δa are the contribution values of the five drivers of the LCN, respectively. $K_{u/c/e/p/a}$ represents the corresponding contribution rate.

3. Results

3.1. Analysis of Land-Use Spatio-Temporal Pattern

As shown in Figures 3 and 4, the land-use of the CUA varied significantly from 2000 to 2020. The areas of grassland and farmland decreased by 9456.25 km^2 and 4262.51 km^2, respectively. The areas of forest land and built-up land increased by 7022.26 km^2 and 5078.67 km^2, respectively. From the perspective of variation time, the areas of built-up land and forest land expanded rapidly after 2010 and 2015, accounting for 76.96% and 95.19% of their total area variation, respectively. The area of grassland significantly decreased since 2015, accounting for 96.43% of its total area variation. The area of farmland continuously reduced during the study period, and a large amount of the reduction occurred from 2010 to 2015. From the perspective of geographical space, the land-use change was markedly concentrated in the CDP-EZ, the SS-EZ, the NES-EZ, and the urban area of Chongqing. The increase in built-up land areas mainly occurred in the CDP-EZ and SS-EZ, and the increase in forest land and grassland areas mainly appeared in the middle east of the CUA.

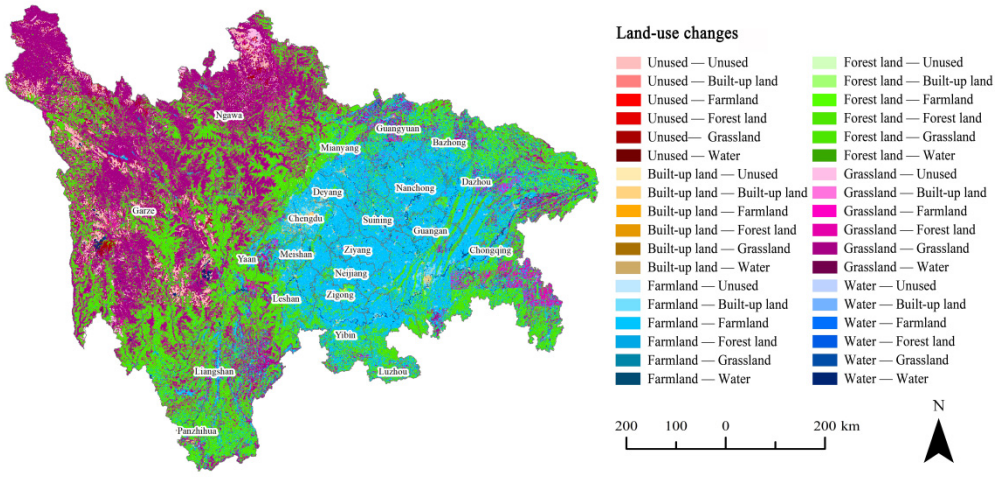

Figure 3. Land-use changes in the CUA from 2000 to 2020.

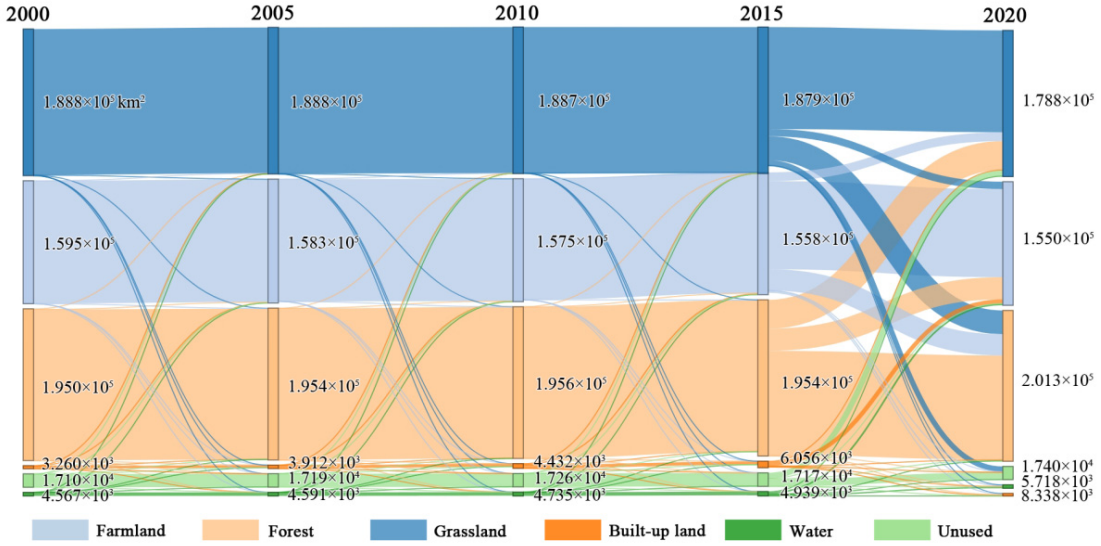

Figure 4. Sankey map of the land-use changes in the CUA from 2000 to 2020.

3.2. Analysis of Spatio-Temporal Evolution Characteristics for LCN

3.2.1. Characteristics of Temporal Variation

As can be seen in Table 3, the LCN in the CUA increased continuously, rising from 3243.96 × 10^4 tons in 2000 to 9700.50 × 10^4 tons in 2020. Prior to 2010, the LCN experienced a rapid growth rate of 9.38%. However, after 2010, the growth rate decelerated, with an average annual growth rate of only 2.01%. Similar to other major urban agglomerations in China, built-up land was the most significant CE land-use type [12,20]. It accounted for over 94% of the total CEs within the CUA throughout the study period. The dual functional attributes of CEs and CSs for farmland were considered in this study. According to the calculation, the LCN of farmland remained negative throughout the study period, indicating that farmland has a net CS effect. Before 2015, its LCN continuously increased, but subsequently decreased. Forest land was always the most significant CS land-use type in the CUA. Its CS contribution rate exceeded 60% and significantly increased since 2015. The CSs of grassland could not be ignored, but it apparently decreased with the area reduction after 2015.

Table 3. LCN in the CUA from 2000 to 2020.

Land-Use Type	LCN/$\times 10^4$ t				
	2000	2005	2010	2015	2020
Built-up land	5045.77	7683.06	9692.38	10,798.23	11,547.52
Farmland	−544.33	−524.15	−481.40	−456.95	−484.33
Forest land	−1106.90	−1108.05	−1108.93	−1107.58	−1212.73
Grassland	−128.94	−128.97	−129.17	−129.02	−122.72
Water	−20.78	−20.99	−21.73	−22.84	−26.37
Unused	−0.85	−0.86	−0.86	−0.86	−0.87
Total	3243.96	5900.04	7950.28	9080.97	9700.50

3.2.2. Characteristics of Spatial Pattern Evolution

- Spatial distribution characteristics

Figure 5 illustrates the LCN distribution in the CUA from 2000 to 2020. The overall spatial pattern of the LCN in the CUA was characterized by higher values in the east and lower values in the west. For the various cities, the LCN exhibited an upward trend, with a stable yet uneven spatial distribution. Chengdu and Chongqing were the core high-value areas of the LCN. The LCN of these two cities were 2044.68 × 10^4 tons and 3059.00 × 10^4 tons in 2020, accounting for 21.08% and 31.53% of the LCN for the entire study area, respectively. As the powerful engines of economic development for the CUA, Chengdu and Chongqing were densely populated and economically active. Their LCN were significantly higher than those of the surrounding areas, and the spatial radiation effect in these areas gradually strengthened as well [42]. The NWS-EDZ is a part of the Qinghai Tibet Plateau and the Hengduan Mountains, endowed with rich forest and grass resources. It is the main CS functional zone in the CUA. The CEs in the NWS-EDZ were completely offset by its CSs in 2000, resulting in an LCN of −129.39 × 10^4 tons. However, the CEs gradually increased over time, and the LCN became positive. Garze was the only region with a consistently negative LCN throughout the study period.

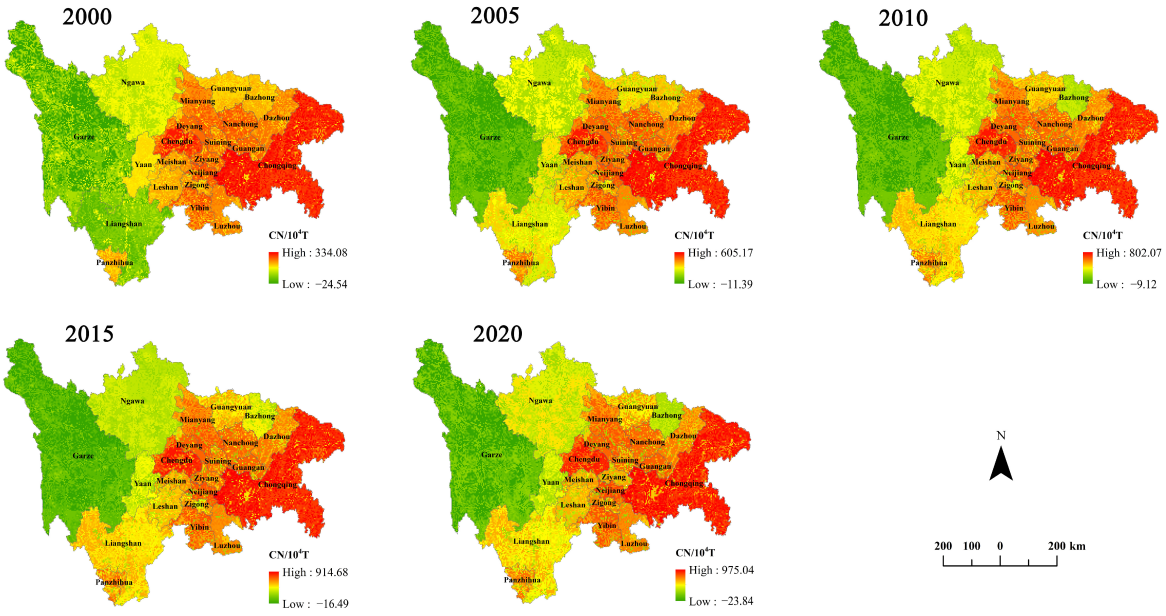

Figure 5. LCN distribution in the CUA from 2000 to 2020.

- Spatial variation characteristics

As shown in Figure 6 and Table 4, the variation of the gravity center orientation for the LCN in the CUA was not significant from 2000 to 2020. However, its distribution center ex-

perienced a substantial spatial migration, shifting from the northwest corner of Chongqing (105°50′43″ E, 30°15′46″ N) to the boundary of Suining (105°37′53″ E, 30°12′53″ N). Specifically, the distribution center of the LCN moved 20.53 km westward and 5.33 km southward, with a total variation distance of 25.81 km. Meanwhile, the long-half axis, short-half axis, area, and perimeter of the standard ellipse increased by 9.12%, 4.49%, 14.02%, and 7.50% throughout the study period, respectively. These phenomena indicated that the spatial distribution pattern of the LCN further expanded from the northeast to the southwest. In addition, the oblateness slightly increased, indicating that the expansion in the east–west direction was relatively greater than that in the north–south direction.

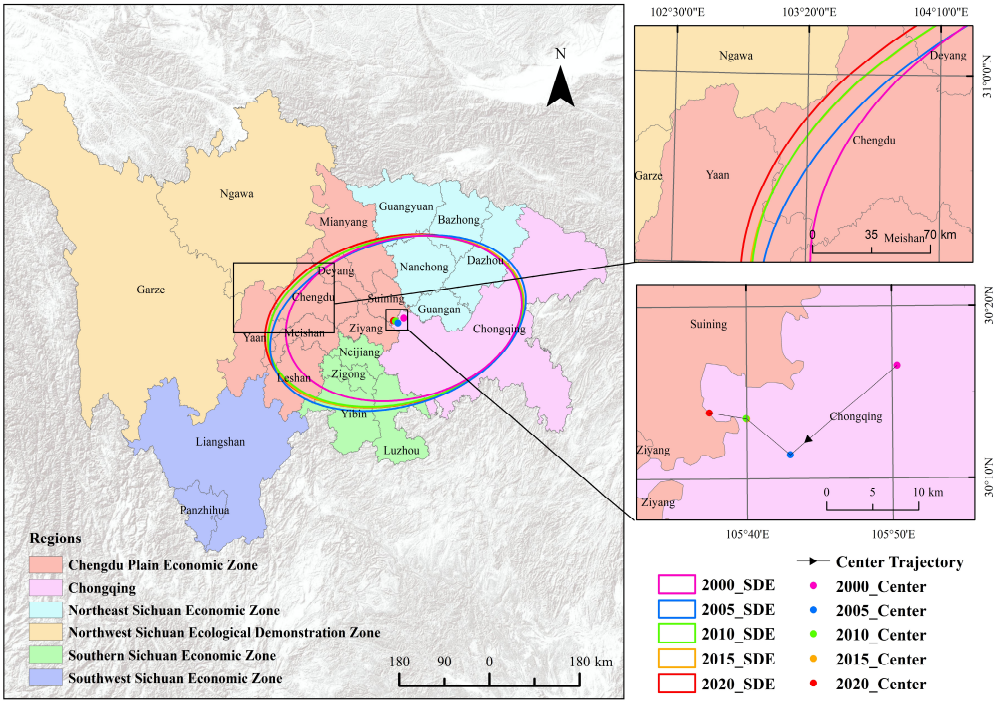

Figure 6. Distribution of the SDE and the shift trajectory of gravity center.

Table 4. SDE parameters of LCN in the CUA from 2000 to 2020.

Year	The Coordinate of Gravity Center			Long-Half Axis/km	Short-Half Axis/km	Oblateness	Area/km^2	Perimeter/km
	Orientation/°	Center X	Center Y					
2000	77.14	105°50′43″	30°15′46″	238.95	159.81	0.33	119,956.45	1265.07
2005	72.48	105°43′32″	30°10′27″	262.54	164.24	0.37	135,452.92	1358.58
2010	76.65	105°40′24″	30°12′34″	258.48	164.02	0.37	133,185.85	1343.95
2015	75.85	105°40′28″	30°12′32″	260.41	164.68	0.37	134,717.17	1352.42
2020	77.07	105°37′53″	30°12′53″	260.74	166.99	0.36	136,774.87	1359.89

- Spatial clustering characteristics

During the period of 2000–2020, the LCN in the CUA generally exhibited significant spatial clustering, as shown in Figure 7. The high–high clusters were mainly concentrated in Chongqing, Chengdu, and Mianyang, which are economic activity centers with high urbanization rates. These cities have frequent industrial and transportation activities, and therefore, exhibit high LCN values. The low–low clusters were mainly concentrated in the NWS-EDZ and some parts of Ya'an and Bazhong. These regions have a high proportion of forest land with strong CS potential and low levels of economic development and industrialization; thus, they maintain relatively low LCN values. There was a significant shift in the distribution of high–low outliers from the south to the north in the CUA throughout the study period. Specifically, the concentration area of the high–low outliers

shifted from Liangshan to south of Leshan, and then to the whole of Leshan, Zigong, and Ngawa. These regions experienced a rapid development of the secondary industry during the period of the low–high outliers, thus leading to a gradual highlighting of the LCN gap within the adjacent areas. The low–high outliers were sporadically distributed from 2000 to 2020. They mainly concentrated along the Yellow River and the other river basins in Chongqing. Due to environmental protection policies, these areas showed low LCN values and were different from the surrounding areas.

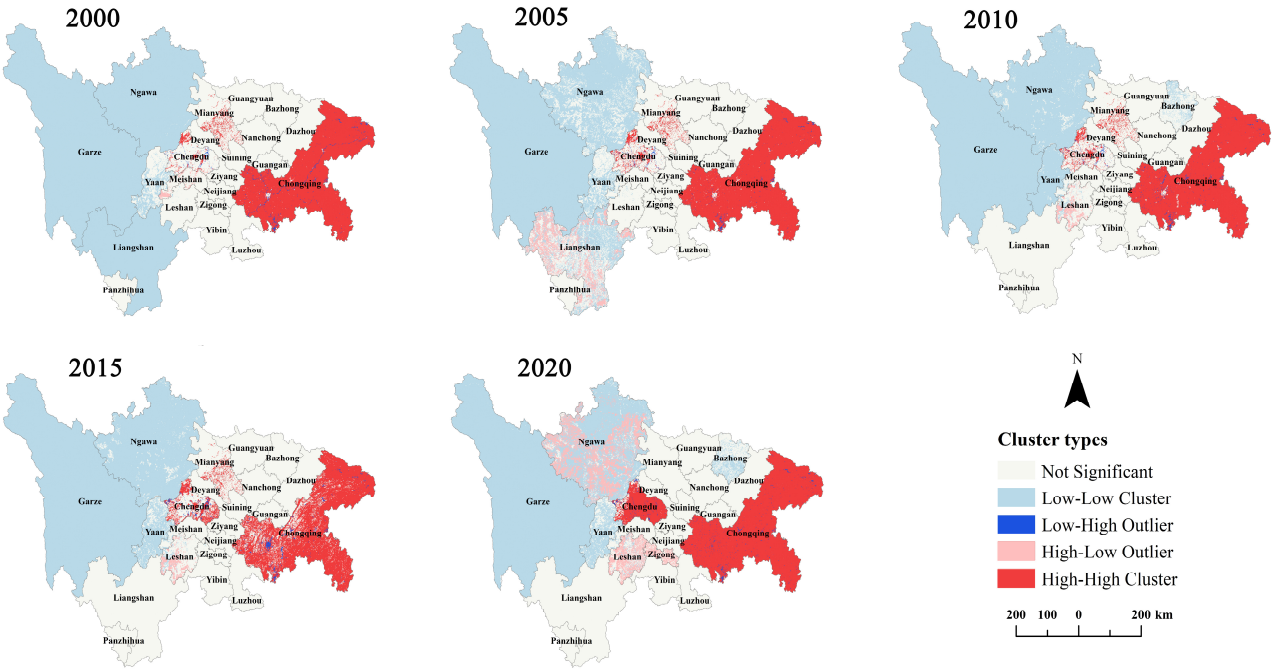

Figure 7. Spatial clustering characteristics of LCN in the CUA from 2000 to 2020.

3.3. Analysis of Land-Use Carbon Balance Pattern

As can be seen in Figure 8, the overall spatial distribution pattern of the ECC in the CUA was high in the east and low in the west. Specifically, the ECC of the various cities were significantly different. Chengdu and Zigong showed a much higher ECC than the others, indicating that they had a relatively high CEs economic benefit. During the study period, the carbon productivity of the cities with a high-value ECC, including Chengdu, Zigong, Deyang, and Ziyang, gradually decreased, while most of the other cities showed an upward trend. This phenomenon illustrated that the development gaps of carbon productivity among the cities gradually narrowed. The spatial distribution pattern of the ESC in the CUA was low in the east and high in the west, which was exactly opposite to that of the ECC (Figure 9). The ESC of the NWS-EDZ and Liangshan continuously exceeded five, demonstrating high carbon compensation rates. Because of the abundant forest and grass resources, these regions have high CS capabilities. The ESC of Chengdu, Deyang, Neijiang, and Guang'an were always less than one. Notably, the ESC of Chengdu and Deyang continuously decreased, while the other cities experienced varying degrees of growth. This phenomenon indicated that the disparity in carbon compensation rates between the cities gradually narrowed.

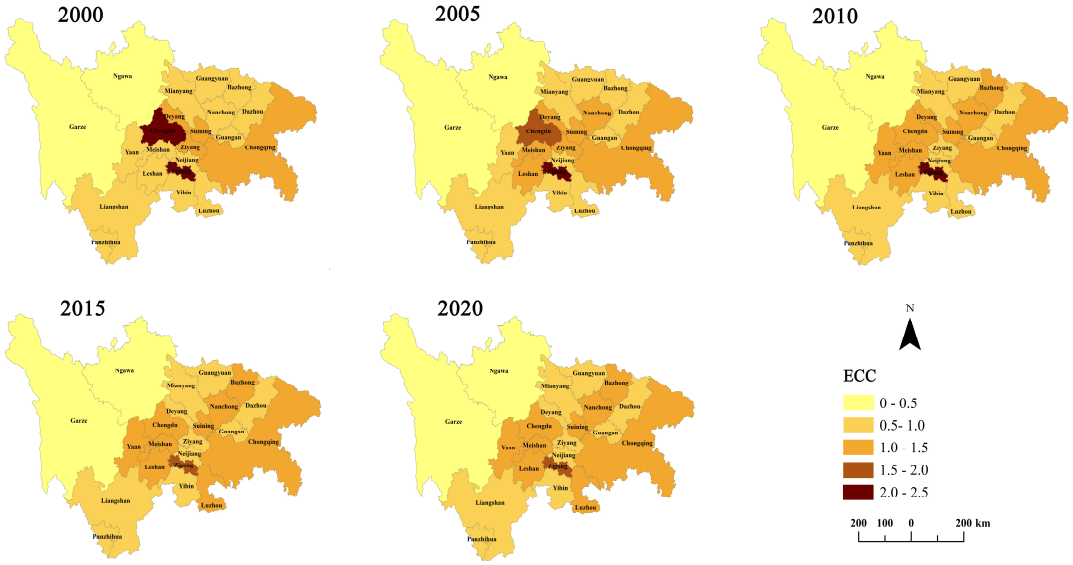

Figure 8. Spatial distribution pattern of ECC in the CUA from 2000 to 2020.

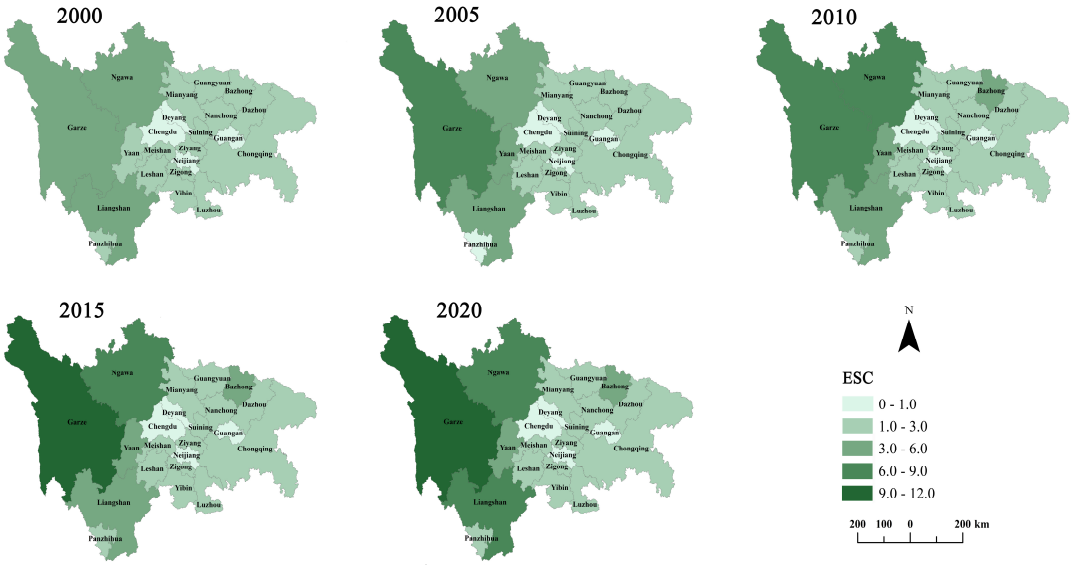

Figure 9. Spatial distribution pattern of ESC in the CUA from 2000 to 2020.

3.4. Analysis of Drivers for LCN

As shown in Table 5, during the period of 2000–2020, the economic development level and built-up land scale positively influenced the LCN in the CUA, while the energy consumption intensity and population density had an inhibitory effect. The impact of the energy use structure on the LCN fluctuated over time. The findings in this study aligned with those of the previous studies, with economic development level being the primary facilitator of LCN in various urban agglomerations or economic zones [25,43,44], and the promotional effect in the CUA was the most pronounced [45]. Its contribution rate was 223.80%. Its contribution amounted to 14,449.47 $\times$ 10^4 tons, which exceeded the sum of the contribution values of all the negative drivers. In the period of 2005–2010, the promotional effect of economic development level on the LCN peaked and then weakened over time. The energy consumption intensity was the primary inhibitor of the LCN. Its contribution was -7702.13×10^4 tons with a rate of 119.29%. The inhibitory effect on the LCN increased steadily over time.

Table 5. Contributions of drivers of LCN in the CUA from 2000 to 2020.

Index		Energy Use Structure	Energy Consumption Intensity	Economic Development Level	Population Density	Built-Up Land Scale
	Note / Year	Δu	Δc	Δe	Δp	Δa
Contribution value /×10⁴ t	2000–2005	405.24	−579.02	2759.07	−733.31	804.10
	2005–2010	−1563.97	−2058.47	5737.21	−1202.68	1138.15
	2010–2015	−544.77	−3430.68	4811.22	−2728.18	3023.10
	2015–2020	43.04	−4170.19	3762.62	−2595.00	3191.07
	2000–2020	−862.24	−7702.13	14,449.47	−5724.41	6295.86
	Note / Year	K_u	K_c	K_e	K_p	K_a
Contribution rate /%	2000–2005	15.26	−21.00	103.88	−27.61	30.27
	2005–2010	−76.28	−100.40	279.83	−58.66	55.51
	2010–2015	−48.18	−303.41	425.51	−241.28	267.37
	2015–2020	69.58	−673.13	607.34	−418.87	515.08
	2000–2020	−13.35	−119.29	223.80	−88.66	97.51

Figure 10 illustrates the contribution values of the LCN drivers across various cities in the CUA throughout the study period. The impacts of the drivers on the LCN in various cities were basically consistent with those observed across the entire study area. However, the impact degrees varied depending on the LCN in different regions. The attenuation of the positive influence of economic development level on the LCN was predominantly observed in Chengdu, Deyang, Luzhou, Zigong, and Chongqing after 2010. The regions where the inhibitory effect of the energy consumption intensity on the LCN notably increased were Chongqing and the Chengdu-Deyang-Mianyang economic belt.

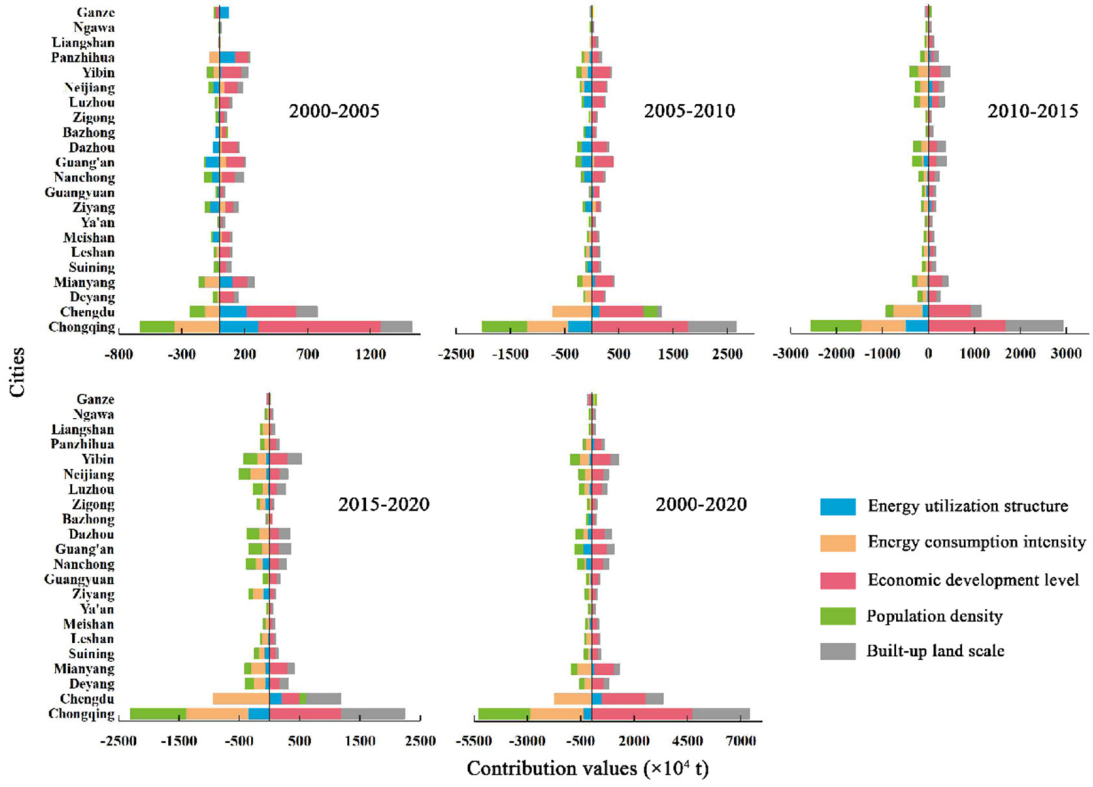

Figure 10. Contribution values of LCN drivers for various cities in the CUA from 2000 to 2020.

4. Discussion

4.1. Alignment Among CEs, Socio-Economic Development, and Ecological Environment

Based on the results in Sections 3.2.1 and 3.3, the disparities in carbon productivity and the carbon compensation rate across the cities gradually narrowed from 2000 to 2020 (Figures 8 and 9), and the growth rate of the LCN in the CUA decelerated after 2010 (Table 3). These phenomena indicated the improving trend of the alignment among the regional CEs, socio-economic development, and ecological environmental governance. During the study period, the secondary and tertiary industries in the CUA experienced rapid growth, and technological advancements continued [46]. Particularly, the industries led by high-end manufacturing and new energy sectors rapidly developed. In addition, the cultivated land quality and efficiency improved in the CUA. Therefore, the process of carbon reduction was accelerated, and the overall carbon productivity was effectively improved. Furthermore, a series of ecological projects led to a significant increase in the forest land area in the CUA and effectively enhanced the regional CS potential (Figure 3). Consequently, integrated ecological environmental governance was realized. However, the carbon-intensive industries like metallurgy, equipment manufacturing, and transportation, gradually expanded along the Chengdu-Deyang-Mianyang economic belt, leading to a reduction in the carbon compensation rates in some areas (Figure 9). This underscored the need for further ecological protection measures. In addition, owing to the industry's vast scale and the inherent complexity of its systems, the process of industrial relocation and integration was intricate [47]. Thus, there existed a decreasing trend of carbon productivity in several cities undergoing industrial transfer (Figure 8).

4.2. Influence Mechanisms of Drivers for LCN

The results based on Section 3.4 showed that the promotional effect of economic development level on the LCN peaked in the period of 2005–2010 (Table 5). This was primarily due to the implementation of the 11th Five-Year Plan for Western Development in 2007, which explicitly outlined the establishment of an economic zone within the CUA. Consequently, the energy-intensive industries, including heavy industry, manufacturing, and transportation, experienced rapid growth and drove the expansion of the regional economy. This resulted in a surge in energy consumption and carbon emissions. During the 12th Five-Year Plan period, the secondary industry rapidly developed, with an average annual growth rate of 9.90% in added value. Concurrently, the national requirements for accelerating industrial technology upgrades and emission reductions were actively responded to in this region [42]. The industrial and energy consumption structure of Chongqing, the CDP-EZ, and the SS-EZ were effectively streamlined. Therefore, the promotional effect of the economic development level on the LCN gradually weakened after 2010.

Conversely, the promotional effect of built-up land scale on the LCN rose sharply after 2010, with an average annual growth rate of 11.33%. This trend was particularly pronounced in the CDP-EZ and SS-EZ (Figure 10). On the one hand, built-up land expanded 76.96% of its total area variation after 2010 (Section 3.1), and substantial amounts of materials and energy were utilized accordingly, contributing to the ongoing rise in CEs from built-up land. On the other hand, the relentless growth of the built-up land areas inevitably resulted in a decrease in the areas of CS land-use types, primarily encompassing forest land and grassland. This aligned with the outcomes of the LCN influenced by the transformations of land-use types (Table 3).

During the study period, the average annual growth rate for the inhibitory effect of energy consumption intensity on the LCN in the CUA was 14.54%. The sustained strengthening trend suggested that technological advancements led to the improvements in energy efficiency. Notably, the average growth rate for the inhibitory effect of the energy consumption intensity on the LCN in Chongqing and the Chengdu-Deyang-Mianyang economic belt was approximately 16% higher than that of the other cities, indicating that the

regional industrial shifts and technological advancements in this region further enhanced their energy utilization efficiency [48].

The inhibitory effect of population density on the LCN in the CUA could not be ignored (Table 5). The population per unit area of built-up land in the CUA dropped from 8500 person/km^2 in 2000 to 7500 person/km^2 in 2015, resulting in a continuous enhancement of the suppressive influence of population density on the LCN. After 2015, cities such as Chongqing, Chengdu, Mianyang, and Panzhihua, experienced a marked rise in population density. Owing to a substantial migration of rural residents to urban areas, coupled with the movement of urban dwellers towards central cities, the urbanization rate across the CUA increased from 51.68% in 2015 to 60.08% in 2020. Consequently, the suppressive effect of population density on the LCN decreased.

The driving effect of energy utilization structure on the LCN exhibited both positive and negative fluctuations (Table 5), which was possibly attributable to the persistently high proportion of fossil fuels used [41]. Despite the CUA's vigorous development and promotion of new energy industries throughout the 13th Five-Year Plan period, the substantial energy-intensive industries continued to overly depend on energy sources with high CEs, and the development within the study region was uneven as well (Figures 5 and 7).

5. Conclusions and Recommendations

In the context of achieving carbon peaking and carbon neutrality goals, this study presents a comprehensive analysis of the spatio-temporal variation and drivers of the LCN within the CUA from 2000 to 2020, with the following main findings.

The area of built-up land and forest land expanded rapidly, mainly through the transformation of grassland and farmland to built-up land and forest land in the CUA during the study period. Built-up land was the main source of CEs, and was predominantly expanded in the CDP-EZ and SS-EZ. The LCN in the CUA increased continuously, although the growth rate decelerated post-2010. The overall spatial distribution of the LCN displayed a characteristic of higher values in the east and lower values in the west, accompanied by pronounced clustering. Chengdu and Chongqing emerged as the central high-value hubs for the LCN, with their spatial radiation effects progressively intensifying. The disparities in carbon productivity and the carbon compensation rate among the cities gradually narrowed from 2000 to 2020. The alignment among the regional CEs, socio-economic development, and ecological environmental governance was effectively improved. Economic development level was the primary facilitator of the LCN. Its promotional effect gradually weakened after 2010, while that of the built-up land scale rose sharply. Energy consumption intensity was the primary inhibitor of the LCN. Its inhibitory effect and the inhibitory effect of population density generally showed an increasing trend.

Drawing from the above findings, the following recommendations are put forth. Firstly, strict control should be exercised over the urban development boundaries and the inefficient expansion of built-up land to foster land conservation and promote intensive use. Meanwhile, efforts to restore farmland should be methodically advanced across various regions, aiming to achieve a balance between the use and restoration of farmland. Secondly, in order to promote low-carbon, balanced development in the entire CUA, it is recommended to optimize the energy structures by enhancing the proportion of clean energy used, and to deepen regional cooperation and coordinated development by strengthening the interactions between the regional central cities and collaborative innovation between the cities and the adjacent regions. Thirdly, to comprehensively enhance the quality of the regional ecological environment and the ecological CS potential, the policy for creating a National Forest City should be promoted and implemented more effectively. Alongside this, the intensification of ecological monitoring and governance in the regions with high CEs should be strengthened.

This research still has several shortcomings that require further study in the future. Firstly, the constant data, including the CE and CS coefficients for various land-use types, were sourced from previous studies. Further investigations are needed across various

regions to enhance the accuracy of these parameters, and the LCN calculations for the different regions should be refined and verified accordingly. Secondly, the five drivers and the underlying influence mechanisms were evaluated in this study; however, the decomposition model can be optimized by introducing additional drivers, such as industrial structure and technological level, to deepen future research.

Author Contributions: Conceptualization, W.W. and X.W.; methodology, W.W. and L.W.; software, W.W.; validation, Z.Z.; formal analysis, W.W.; resources, X.W.; data curation, W.W. and Z.Z.; writing—original draft preparation, W.W.; writing—review and editing, X.W. and L.W.; visualization, W.W.; supervision, X.W.; project administration, X.W.; funding acquisition, X.W. and D.L. All authors have read and agreed to the published version of the manuscript.

Funding: This research was supported by the Strategy Priority Research Program of the Chinese Academy of Sciences (No. XDB0760100) and the Project of the China–Sri Lanka Joint Center for Education and Research of the Chinese Academy of Sciences (No. 133244KYSB20210026).

Data Availability Statement: The original contributions presented in this study are included in the article, further inquiries can be directed to the corresponding authors.

Conflicts of Interest: The authors declare no conflicts of interest.

References

1. Houghton, R.A.; House, J.I.; Pongratz, J.; Van Der Werf, G.R.; Defries, R.S.; Hansen, M.C.; Le Quéré, C.; Ramankutty, N. Carbon emissions from land use and land-cover change. *Biogeosciences* **2012**, *9*, 5125–5142. [CrossRef]
2. IPCC. *Climate Change 2023: Synthesis Report. Contribution of Working Group I, II and III to the Sixth Assessment Report of the Intergovernmental Panel on Climate Change*; Core Writing Team, Lee, H., Romero, J., Eds.; IPCC: Geneva, Switzerland, 2023.
3. IPCC. *Special Report. Climate Change and Land*; IPCC: Geneva, Switzerland, 2019.
4. IPCC. *Climate Change 2014: Mitigation of Climate Change. The Working Group III Contribution to the Fifth Assessment Report of the Intergovernmental Panel on Climate Change*; Cambridge University Press: Cambridge, UK, 2014.
5. IPCC. *Climate Change 2022: Mitigation of Climate Change. The Working Group III Contribution to the Sixth Assessment Report of the Intergovernmental Panel on Climate Change*; Cambridge University Press: Cambridge, UK, 2022.
6. Yang, X.H.; Jin, X.B.; Liu, J.; Gu, Z.M.; Zhou, Y.K. Design and implementation of system estimating carbon emission induced by land use/cover change. *Bull. Surv. Mapp.* **2019**, *4*, 54. (In Chinese)
7. Simmonds, M.B.; Di Vittorio, A.V.; Jahns, C.; Johnston, E.; Jones, A.; Nico, P.S. Impacts of California's climate-relevant land use policy scenarios on terrestrial carbon emissions (CO2 and CH4) and wildfire risk. *Environ. Res. Lett.* **2021**, *16*, 014044. [CrossRef]
8. Parsamehr, K.; Gholamalifard, M.; Kooch, Y.; Azadi, H.; Scheffran, J. Impact of land cover changes on reducing greenhouse emissions: Site selection, baseline modeling, and strategic environmental assessment of REDD+projects. *Land Degrad. Dev.* **2023**, *34*, 2763–2779. [CrossRef]
9. Liu, G.H.; Cui, F.L.; Wang, Y. Spatial effects of urbanization, ecological construction and their interaction on land use carbon emissions/absorption: Evidence from China. *Ecol. Indic.* **2024**, *160*, 111817. [CrossRef]
10. Sun, M.W.; Liang, B.Y.; Meng, X.B.; Zhang, Y.F.; Wang, Z.; Wang, J. Study on the evolution of spatial and temporal patterns of carbon emissions and influencing factors in China. *Land* **2024**, *13*, 828. [CrossRef]
11. Deng, X.K.; Yu, Y.H.; Liu, Y.F. Effect of construction land expansion on energy-related carbon emissions: Empirical analysis of China and its provinces from 2001 to 2011. *Energies* **2015**, *8*, 5516–5537. [CrossRef]
12. Wang, C.; Zhan, J.Y.; Zhang, F.; Liu, W.; Twumasi-Ankrah, M.J. Analysis of urban carbon balance based on land use dynamics in the Beijing-Tianjin-Hebei region, China. *J. Clean. Prod.* **2021**, *281*, 125138. [CrossRef]
13. Padbhushan, R.; Kumar, U.; Sharma, S.; Rana, D.S.; Kumar, R.; Kohli, A.; Kumari, P.; Parmar, B.; Kaviraj, M.; Sinha, A.K.; et al. Impact of land-use changes on soil properties and carbon pools in India: A meta-analysis. *Front. Environ. Sci.* **2022**, *9*, 794866. [CrossRef]
14. Zhang, H.; Peng, Q.R.; Wang, R.; Qiang, W.L.; Zhang, J.X. Tempo-spatial patterns and influencing factors of carbon sequestration in Chinese counties. *J. Ecol.* **2020**, *40*, 8988–8998. (In Chinese)
15. Dai, L.L.; Feng, C.W.; Zhou, Z.J.; Jin, D. Research on the spatio-temporal evolution of carbon balance at the county level in China. *Ecol. Econ.* **2023**, *39*, 31–39. (In Chinese)
16. Gui, D.W.; He, H.G.; Liu, C.M.; Han, S.S. Spatio-temporal dynamic evolution of carbon emissions from land use change in Guangdong Province, China, 2000–2020. *Ecol. Indic.* **2023**, *156*, 111131. [CrossRef]
17. IPCC. *Climate Change 2007: The Physical Science Basis. The Working Group I Contribution to the Fourth Assessment Report of the Intergovernmental Panel on Climate Change*; Cambridge University Press: Cambridge, UK, 2008.
18. Wang, R.; Feng, Y. Research on China's ecological welfare performance evaluation and improvement path from the perspective of high-quality development. *Math. Probl. Eng.* **2020**, *2020*, 5476089. [CrossRef]

19. Zhang, C.Y.; Zhao, L.; Zhang, H.; Chen, M.N.; Fang, R.Y.; Yao, Y.; Zhang, Q.P.; Wang, Q. Spatial-temporal characteristics of carbon emissions from land use change in Yellow River Delta region, China. *Ecol. Indic.* **2022**, *136*, 108623. [CrossRef]
20. Zhang, N.; Sun, F.C.; Hu, Y.L.; Tang, Q. Regional difference and spatial convergence of land use carbon emissions in three major urban agglomerations of Yangtze River Economic Belt. *Environ. Sci.* **2024**, *45*, 4656–4669. (In Chinese)
21. Qin, H.; Huang, Q.; Zhang, Z.; Lu, Y.; Li, M.; Xu, L.; Chen, Z. Carbon dioxide emission driving factors analysis and policy implications of Chinese cities: Combining geographically weighted regression with two-step cluster. *Sci. Total Environ.* **2019**, *684*, 413–424. [CrossRef]
22. Su, K.; Wei, D.Z.; Lin, W.X. Influencing factors and spatial patterns of energy-related carbon emissions at the city-scale in Fujian province, southeastern China. *J. Clean. Prod.* **2020**, *244*, 118840. [CrossRef]
23. Hu, M.; Sarwar, S.; Li, Z. Spatio-temporal differentiation mode and threshold effect of yangtze river delta urban ecological well-being performance based on network DEA. *Sustainability* **2021**, *13*, 4550. [CrossRef]
24. Aziz, S.; Chowdhury, S.A. Analysis of agricultural greenhouse gas emissions using the STIRPAT model: A case study of Bangladesh. *Environ. Dev. Sustain.* **2023**, *25*, 3945–3965. [CrossRef]
25. Chen, J.S.; Zhang, J.J.; Li, J.L.; Li, S. Spatio-temporal pattern changes and driving factors of carbon emissions in the Beijing-Tianjin-Hebei region. *J. Ecol.* **2024**, *44*, 2270–2283. (In Chinese)
26. Nieves, J.A.; Aristizábal, A.J.; Dyner, I.; Báez, O.; Ospina, D.H. Energy demand and greenhouse gas emissions analysis in Colombia: A LEAP model application. *Energy* **2019**, *169*, 380–397. [CrossRef]
27. Fan, R.; Zhang, X.; Bizimana, A.; Zhou, T.; Liu, J.S.; Meng, X.Z. Achieving China's carbon neutrality: Predicting driving factors of CO2 emission by artificial neural network. *J. Clean. Prod.* **2022**, *362*, 132331. [CrossRef]
28. Wang, H.; Jin, Y.J.; Hong, X.M.; Tian, F.; Wu, J.; Nie, X. Integrating IPAT and CLUMondo models to assess the impact of carbon peak on land use. *Land* **2022**, *11*, 573. [CrossRef]
29. Xia, C.Y.; Zhang, J.; Zhao, J.; Xue, F.; Li, Q.; Fang, K.; Shao, Z.; Zhang, J.; Li, S.; Zhou, J. Exploring potential of urban land-use management on carbon emissions-a case of Hangzhou, China. *Ecol. Indic.* **2023**, *146*, 109902. [CrossRef]
30. Li, Z.N.; Yang, Y.; Zhu, X.D. Spatio-temporal differences in carbon emissions and carbon balance zoning in Jiangsu Province based on land-use change. *Environ. Prot. Sci.* **2024**, *50*, 120–132. (In Chinese)
31. Liu, M.; Yang, L. Spatial pattern of China's agricultural carbon emission performance. *Ecol. Indic.* **2021**, *133*, 108345. [CrossRef]
32. Wang, Y.F.; Liang, S.; Liang, Y.X.; Liu, X.X. A Comprehensive accounting of carbon emissions and carbon sinks of China's agricultural sector. *Land* **2024**, *13*, 1452. [CrossRef]
33. Fang, J.Y.; Guo, Z.D.; Piao, S.L.; Chen, A.P. Estimation of land vegetation carbon sequestration in China from 1981 to 2000. *Chin. Sci. (Vol. D Earth Sci.)* **2007**, *6*, 804–812. (In Chinese)
34. Fang, J.; Yu, G.; Liu, L.; Hu, S.; Chapin, F.S., III. Climate change, human impacts, and carbon sequestration in China. *Proc. Natl. Acad. Sci. USA* **2018**, *115*, 4015–4020. [CrossRef]
35. Kong, D.S.; Zhang, H. Ecological service function value assessment of Zhangye Heihe Wetland Nature Reserve. *J. Ecol.* **2015**, *35*, 972–983. (In Chinese)
36. Chen, L.H.; Hang, Y.H.; Li, Q.F. Spatial-temporal characteristics and influencing factors of carbon emissions from land use and land cover in black soil region of Northeast China based on LMDI simulation. *Sustainability* **2023**, *15*, 9334. [CrossRef]
37. Ang, B.W. The LMDI approach to decomposition analysis: A practical guide. *Energy Policy* **2005**, *33*, 867–871. [CrossRef]
38. Yang, D.; Luan, W.X.; Qiao, L.; Pratama, M. Modeling and spatio-temporal analysis of city-level carbon emissions based on nighttime light satellite imagery. *Appl. Energy* **2020**, *268*, 114696. [CrossRef]
39. Wang, Q.; Su, M. The effects of urbanization and industrialization on decoupling economic growth from carbon emission-a case study of China. *Sustain. Cities Soc.* **2019**, *51*, 101758. [CrossRef]
40. Zhang, L.; Mu, R.Y.; Zhan, Y.F.; Yu, J.F.; Liu, L.F.; Yu, Y.H.; Zhang, J.X. Digital economy, energy efficiency, and carbon emissions: Evidence from provincial panel data in China. *Sci. Total Environ.* **2022**, *852*, 158403. [CrossRef] [PubMed]
41. Xu, M.; Yang, X.; Deng, L.L.; Liao, X.; Niu, Z.S.; Hao, L. Decoupling state of urban development and carbon emissions and its driving factors and predictions: A case study of Chengdu metropolitan area. *Ecol. Inform.* **2024**, *82*, 102692. [CrossRef]
42. Zhang, J.; Lu, H.; Peng, W.F.; Zhang, L.D. Analyzing carbon emissions and influencing factors in Chengdu-Chongqing urban agglomeration counties. *J. Environ. Sci.* **2025**, *151*, 640–651. [CrossRef]
43. Jiang, P.; Gong, X.; Yang, Y.; Tang, K.; Zhao, Y.; Liu, S.; Liu, L. Research on spatial and temporal differences of carbon emissions and influencing factors in eight economic regions of China based on LMDI model. *Sci. Rep.* **2023**, *13*, 7965. [CrossRef] [PubMed]
44. Luo, X.C.; Liu, C.K.; Zhao, H.H. Driving factors and emission reduction scenarios analysis of CO2 emissions in Guangdong-Hong Kong-Macao Greater Bay Area and surrounding cities based on LMDI and system dynamics. *Sci. Total Environ.* **2023**, *870*, 161966. [CrossRef]
45. Liu, Y.X.; He, S.; Jiang, Y.J.; Luo, X.; Yuan, J.H. Research on the spatio-temporal decomposition of driving factors for carbon emissions in China's four major urban agglomerations. *Clim. Change Res.* **2024**, *20*, 231–241. (In Chinese)
46. Zeng, H.B.; Shao, B.L.; Bian, G.Q.; Dai, H.B.; Zhou, F.Y. Analysis of influencing factors and trend forecast of CO2 emission in Chengdu-Chongqing urban agglomeration. *Sustainability* **2022**, *14*, 1167. [CrossRef]

47. Wang, Z.F.; Cai, Y.W.; Luo, S.W.; Yang, Y.F. Analysis of spatio-temporal trends and influencing factors of carbon emissions in the Chengyu urban agglomeration. *Environ. Sci. Technol.* **2023**, *46*, 205–215. (In Chinese)
48. Lai, D.L.; Hu, Y.; Wang, Y.G. Analysis of spatio-temporal heterogeneity and influencing factors of land-use carbon emissions in the Chengyu urban agglomeration. *J. Mianyang Norm. Univ. (Nat. Sci. Educ.)* **2023**, *42*, 97–105. (In Chinese)

Disclaimer/Publisher's Note: The statements, opinions and data contained in all publications are solely those of the individual author(s) and contributor(s) and not of MDPI and/or the editor(s). MDPI and/or the editor(s) disclaim responsibility for any injury to people or property resulting from any ideas, methods, instructions or products referred to in the content.